

# Computational periodicity as observed in a simple system

By EDWARD N. LORENZ, *Department of Earth, Atmospheric, and Planetary Sciences, Massachusetts Institute of Technology, Cambridge, MA 02139, USA*

(Manuscript received 2 February 2006; in final form 26 June 2006)

## ABSTRACT

When the exact time-dependent solutions of a system of ordinary differential equations are chaotic, numerical solutions obtained by using particular schemes for approximating time derivatives by finite differences, with particular values of the time increment  $\tau$ , are sometimes stably periodic. It is suggested that this phenomenon be called *computational periodicity*.

A particular system of three equations with a chaotic exact solution is solved numerically with an  $N$ th-order Taylor-series scheme, with various values of  $N$ , and with values of  $\tau$  ranging from near zero to just below the critical value for computational instability. When  $N = 1$ , the value of  $\tau$  below which computational periodicity never appears is extremely small, and frequent alternations between chaos and periodicity occur within the range of  $\tau$ . Computational periodicity occupies most of the range when  $N = 2$  or 3, and about half when  $N = 4$ .

These solutions are compared with those produced by fourth-order Runge–Kutta and Adams–Bashforth schemes, and with numerical solutions of two other simple systems. There is some evidence that computational periodicity will more likely occur when the chaos in the exact solutions is not very robust, that is, if relatively small changes in the values of the constants can replace the chaos by periodicity.

## 1. Introduction

When seeking time-dependent numerical solutions of systems of differential equations (DEs), one is faced with a choice of procedures for approximating the time derivatives by finite differences. Partial DEs are generally considered appropriate when modeling atmospheric or oceanic flow, and here one sometimes merges the time differencing and space differencing into a single more elaborate scheme. Particularly in operational weather forecasting, new procedures, often tailored to the particular equations, are continually being introduced; a very recent example is a semi-implicit scheme of Giraldo (2005). When one chooses a rather simple system of ordinary DEs for a model, however, one is likely to use a relatively simple differencing method, particularly when beginning to investigate a new system. The familiar Runge–Kutta and Adams–Bashforth methods are described in textbooks written well before electronic computers were generally available to use them (e.g. von Karman and Biot, 1940). Formulas for these and other schemes, some more recently developed, have been presented in tabular form by Durran (1999), who also discusses their adequacy for use in geophysical problems. This study is concerned only with approximations to ordinary DEs.

Anyone who has solved many systems of equations numerically will be familiar with the phenomenon of computational instability (CI), where the computed values of the dependent variables eventually go rapidly to infinity. The often cited Courant–Friedrichs–Lewy conditions (Courant et al., 1928) apply to partial DEs, but one of their implications, that the chosen time increment  $\tau$  cannot be too large a fraction of the period of any possible oscillation if CI is to be avoided, is equally true for ordinary DEs. The usual cure for CI consists of simply lowering  $\tau$ , but sometimes there is a range where  $\tau$  is small enough to prevent CI, but where the numerically determined solution nevertheless bears little resemblance to the solution that is being sought. In particular, when the exact solution varies periodically with time, there is sometimes a range of  $\tau$  where the computed solution is chaotic. This phenomenon has been called *computational chaos* (CC) (Lorenz, 1989).

A while ago we encountered an instance of the opposite phenomenon. We had recently submitted an article (Lorenz, 2006, hereafter L06) to *Tellus*, dealing with a system whose solution, as estimated by a fourth-order Runge–Kutta scheme with a small time increment, was chaotic, and we had included several pictures of the resulting strange attractor. One reviewer went well beyond the call of duty and attempted to duplicate our pictures, and instead found a stable limit cycle. It presently appeared that he or she had used a first-order time-differencing scheme, which

one might have presumed adequate for detecting chaos. All of the numerical values, including  $\tau$ , were the same as ours, so that the choices of differencing schemes seemed a likely reason for the discrepancy. We proceeded to solve the equations with a first-order scheme, and confirmed the reviewer's findings.

By analogy with CC, it seems reasonable to call this phenomenon, where an exact solution is chaotic and a numerical solution is periodic, *computational periodicity* (CP). The term 'periodicity' is intended to include almost-periodicity, where the solution is expressible as a sum of periodic components with incommensurable periods. It is also intended to exclude systems where all periodic solutions are unstable.

This study deals with CP. Our primary purpose is to observe in detail the conditions under which CP appears in numerical solutions of the particular system where we first encountered it. We shall make some inferences concerning its appearance in more general systems, but we emphasize that no attempt will be made to present a comprehensive treatment.

### 2. First-order differencing

The system on which this study is based consists of the three equations

$$\frac{dX}{dt} = -Y^2 - Z^2 - aX + aF, \tag{1a}$$

$$\frac{dY}{dt} = XY - bXZ - Y + G, \tag{1b}$$

$$\frac{dZ}{dt} = bXY + XZ - Z. \tag{1c}$$

It was originally introduced to illuminate certain properties of the general atmospheric circulation (Lorenz, 1984, hereafter L84), and it has seen considerable subsequent use, often for unrelated purposes (e.g. Trevisan, 1993; Aires and Rossow, 2003). In meteorological applications  $X$  represents the strength of a circumpolar westerly current, while  $Y$  and  $Z$  denote the cosine and sine phases of a superposed chain of large-scale waves. The absence of explicit coefficients of  $Y$  and  $Z$  in eqs. (1b) and (1c) implies that the chosen time unit is the damping time for the waves, assumed to be 5 d.

In the computations that follow we shall use an  $N$ th-order truncated Taylor-series procedure, namely

$$X(t + \tau) = \sum_{n=0}^N \frac{[d^n X(t)/dt^n] \tau^n}{n!}, \tag{2}$$

with analogous expressions for  $Y$  and  $Z$ , chosen because a single very simple program will handle any value of  $N$ . Higher derivatives are easily expressed in terms of lower ones. Interpolation between time steps is accomplished by substituting a fraction of  $\tau$  for  $\tau$  in eq. (2).

With  $a = 1/4$ ,  $b = 4$ ,  $F = 8$ , and  $G = 1$ , the behaviour of eqs. (1) was found in L84 and L06 to be chaotic. Figure 1a shows a cross section of the attractor—its intersection with the state-space plane  $Z = 0$ —as determined by integration for 3 000 000 time steps with  $N = 4$  and  $\tau = 0.025$ , or three hours.

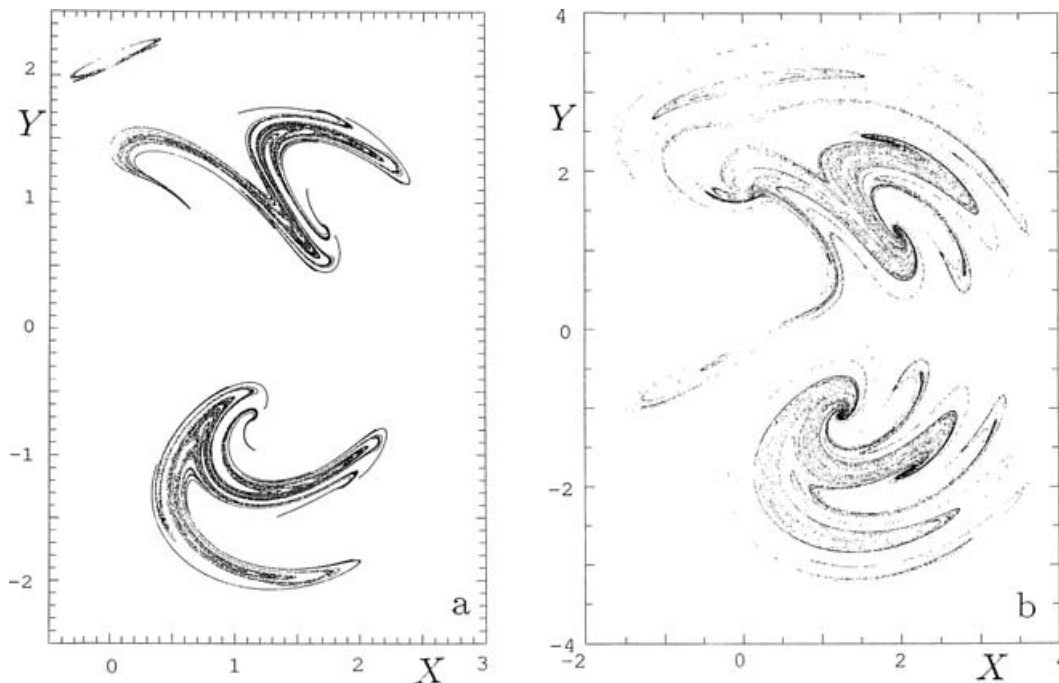


Fig. 1. (a) Intersection with plane  $Z = 0$  of attractor of eqs. (1) when  $a = 1/4$ ,  $b = 4$ ,  $F = 8$  and  $G = 1$ , as represented by 97 428 points computed with fourth-order Taylor-series procedure with time increment  $\tau = 0.025$ . Coordinates are  $X$  and  $Y$ . (b) The same, but with 168 266 points, and when  $a = 1/4$ ,  $b = 5$ ,  $F = 14$  and  $G = 7/4$ . Note the change in scale.

The 97 428 points of intersection comprising the figure were determined by interpolating between steps. Figure 1b shows, on a somewhat compressed scale, a larger and more complicated cross section, similarly produced, again with  $a = 1/4$ , but with the larger values  $b = 5$ ,  $F = 14$  and  $G = 7/4$ . The figures show rather typical low-degree strange attractors—hallmarks of chaos.

Presumably, given  $\tau$ , a larger value of  $N$  better approximates the differential equations, at least when  $\tau$  is moderately small, suggesting that the exact solution of eqs. (1) is indeed chaotic. Presumably also, given  $N$ , a smaller value of  $\tau$  yields a better approximation, suggesting that with  $N = 1$  a low enough value of  $\tau$  will reveal the chaos. Upon making a set of runs with  $N = 1$ , with successively smaller values of  $\tau$ , we encountered chaos only after  $\tau$  had fallen by a factor of nearly 10 from the original 0.025,

to 0.0028. At this point the resulting attractor closely resembled the one in Fig. 1a.

Choosing many values of  $\tau$  and examining each resulting attractor is at best a cumbersome procedure, while choosing fewer values entails the risk of jumping over short ranges of  $\tau$  with anomalous behaviour. An equally reliable indicator of chaos, in a numerical approximation or in the original DEs, is the leading Lyapunov exponent  $\lambda_1$ , which is positive when chaos is present and zero otherwise, except when the solution decays to a steady state, when  $\lambda_1$  is negative. Each new value of  $\tau$  effectively defines a new dynamical system, which may possess a new value of  $\lambda_1$ .

With the values of the constants used in Fig. 1a, the three Lyapunov exponents  $\lambda_1, \lambda_2, \lambda_3$  of the DEs are 0.17, 0.00 and  $-0.39$ . Figure 2a shows the computed values of these exponents,

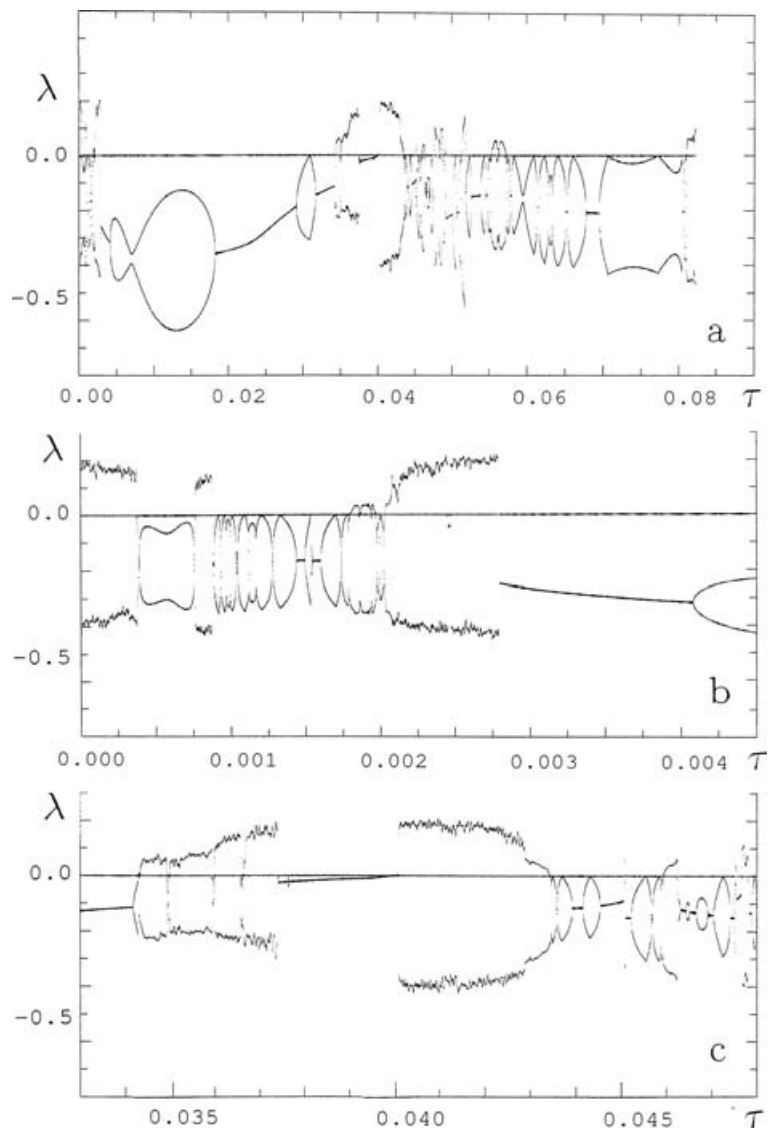


Fig. 2. (a) Superposition of three curves showing variations with  $\tau$ , as  $\tau$  increases from 0 to  $\tau_2$ , of Lyapunov exponents  $\lambda_1, \lambda_2$  and  $\lambda_3$  of approximation to eqs. (1), when  $a = 1/4, b = 4, F = 8$  and  $G = 1$ , by first-order differencing with time increment  $\tau$ . Horizontal coordinate is  $\tau$ . Vertical coordinate is  $\lambda$ . For each value of  $\tau$ , either  $\lambda_1$  or  $\lambda_2$  coincides with zero line. Where fewer than three curves appear, two or more exponents are equal. (b) The section of (a) where  $\tau < 0.0045$ , horizontally stretched 20 times. (c) The section of (a) where  $0.033 < \tau < 0.048$ , horizontally stretched six times.

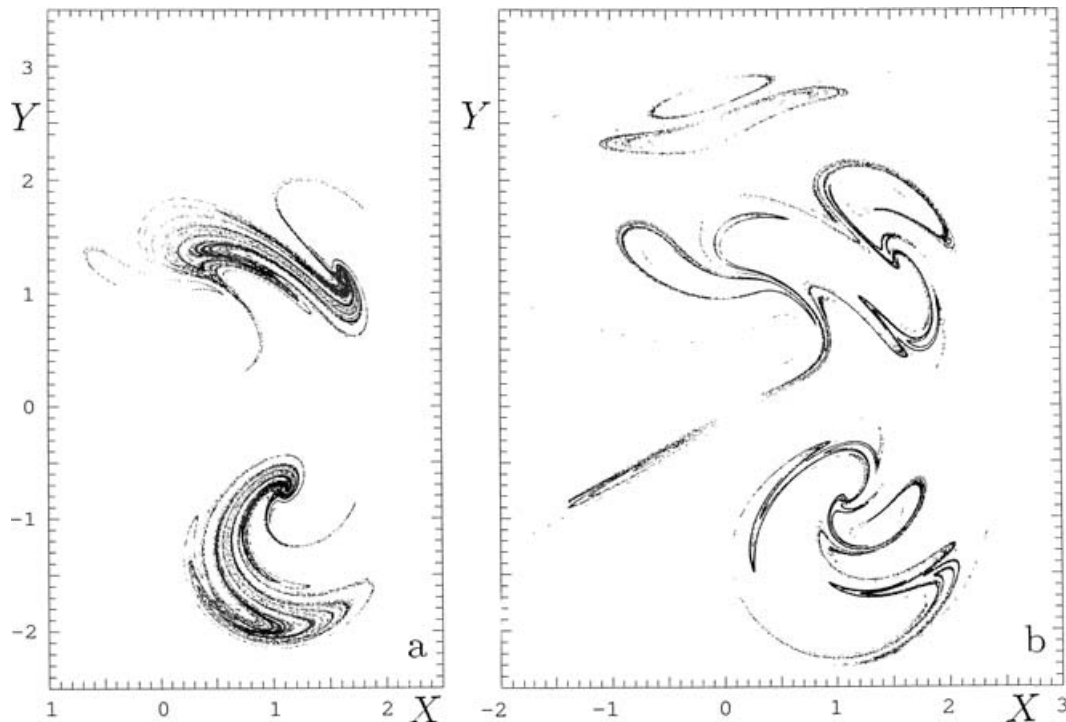


Fig. 3. (a) Intersection with plane  $Z = 0$  of attractor of approximation to eqs. (1), when  $a = 1/4$ ,  $b = 4$ ,  $F = 8$  and  $G = 1$ , by first-order differencing with  $\tau = 0.037$ . Coordinates are  $X$  and  $Y$ . (b) The same, but with  $\tau = 0.042$ .

with  $N = 1$ , as  $\tau$  increases from just above 0 through  $\tau_1$ , the highest value below which only chaos occurs, to  $\tau_2$ , the lowest value above which only CI occurs. Each value is determined from one basic and three perturbed runs, and each run lasts 10 yr, so necessarily the lowest values of  $\tau$  demand many time steps. Evidently  $\tau_2 = 0.0822$ , or about ten hours. We see that CP, where  $\lambda_1 = 0$ , dominates, but does not occupy the whole range from  $\tau_1$  to  $\tau_2$ .

When  $\tau$  is near  $\tau_1$  the resolution in Fig. 2a is poor, and Fig. 2b repeats the extreme left portion, with a stretched horizontal scale. The chaos previously found when  $\tau = 0.0028$  evidently disappears when  $\tau$  becomes still smaller, and does not become permanently established until  $\tau$  reaches 0.00039 ( $=\tau_1$ ), or 2.8 min—a much smaller value than one would ordinarily choose in solving eqs. (1). Above  $\tau_1$ , values of  $\lambda_2$  and  $\lambda_3$  alternate rapidly between being equal and being unequal, indicating rapid alternations in the manner in which small initial departures from the periodic solution will decay.

Returning to Fig. 2a, we see some larger values of  $\tau$  where chaos appears, dominated by a range from 0.0344 to 0.0374 and one from 0.0402 to 0.0435. The details are more easily seen in Fig. 2c, which stretches the central portion of Fig. 2a.

We have found that certain values of  $\tau$  produce intransitivity, that is, with the same  $\tau$ , different initial states may produce different attractors and different values of  $\lambda_1$ ,  $\lambda_2$ ,  $\lambda_3$  and, in particular, one solution may be periodic while another is chaotic. In Fig. 2, where only one set of exponents is shown for each

$\tau$ , the curves were produced by increasing  $\tau$  in small steps, and using the final state from one computation as the initial state in the next. If  $\tau$  had instead been decreased in small steps, additional chaotic ranges would have appeared in Fig. 2c between 0.0444 and 0.0449 and between 0.0453 and 0.0459, while the short chaotic range between 0.0459 and 0.0462 would have disappeared. Something resembling hysteresis thus occurs; without the hysteresis we might have failed to notice the intransitivity.

Figures 3a and b show cross sections of the attractors for  $\tau = 0.037$  and  $\tau = 0.042$ —values within the prominent chaotic ranges in Fig. 2c. Both attractors are clearly strange. Figure 3a looks somewhat like the attractor of the DEs in Fig. 1a, but it is by no means a duplication. Fig. 3b shows a closer resemblance to Fig. 1b, which was produced with different values of the constants. Rather unexpectedly, Fig. 3a fits rather neatly into the interior empty spaces in Fig. 3b; most states encountered when  $\tau = 0.037$  seem to be carefully avoided when  $\tau = 0.042$ .

Quantitatively our results must depend upon the values of the constants. In Fig. 4, we present some similarly constructed curves, again with  $a = 1/4$ ,  $b = 4$  and  $F = 8$ , but with  $G$  successively equalling 1.0, 1.1, 1.2 and 1.3. The details vary considerably, but all exhibit some periodicity extending below  $\tau = 0.01$ , and all show several separate chaotic ranges of  $\tau$  above 0.02. We have verified that qualitatively similar curves also arise when other constants are changed, so that the CP has not resulted from a fortuitous choice.

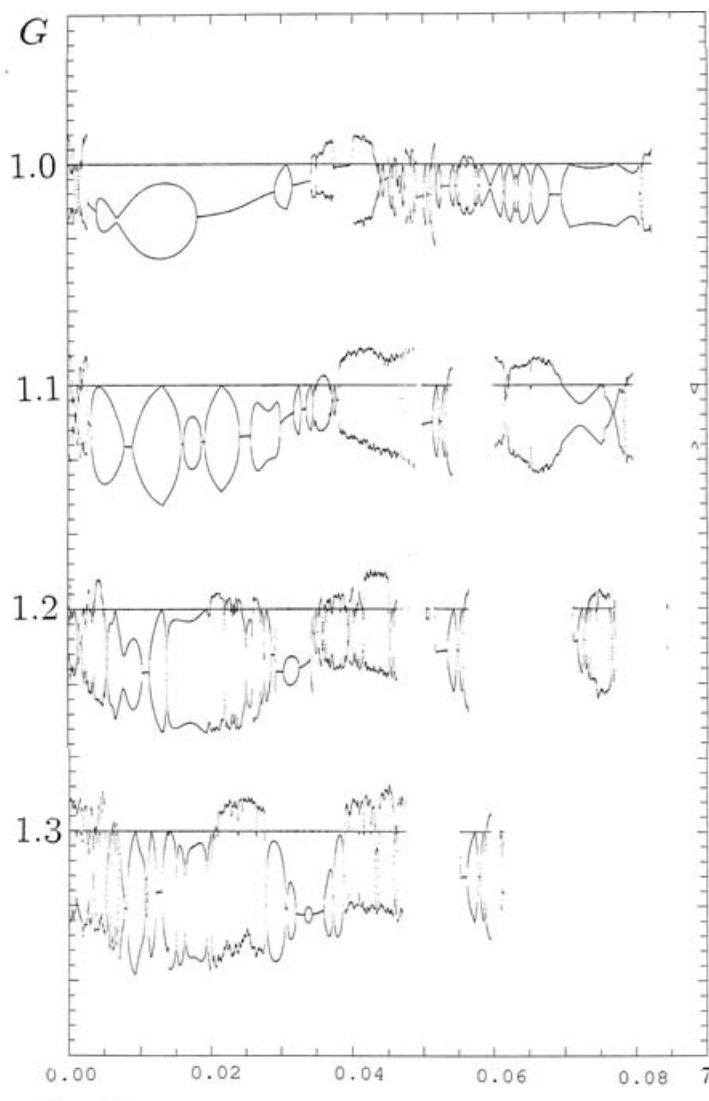


Fig. 4. The same as Fig. 2a, but separately for each value of  $G$  indicated by number at left of curves. Numbers indicating  $G$  are placed opposite zero lines for  $\lambda$ . Small divisions on left and right margins are at intervals of 0.1 unit of  $\lambda$ .

A new feature is the presence of some ranges where no points at all appear, most pronounced when  $G = 1.2$  and  $0.057 < \tau < 0.071$ . Here the numerical solutions are computationally unstable, even though they become stable again before  $\tau$  finally reaches  $\tau_2$ .

Between  $\tau = 0.005$  and  $0.065$  the panels in Fig. 4 for  $G = 1.2$  and  $1.3$  are much alike; clearly the alternations between periodicity and chaos are the same phenomenon in either panel. However, as  $G$  varies from  $1.0$  to  $1.3$  in the DEs, a window—a continuum of values of  $\tau$  where the solution is periodic, within an otherwise generally chaotic range—extends from  $1.186$  to  $1.217$ , and hence spans  $1.2$ . Within this window, the attractor of the DEs is a closed curve, and its intersection with the plane  $Z = 0$  consists of just  $20$  points. The question thus arises as to whether when  $G = 1.2$  the periodicity should be called CP or whether another name is more appropriate, since the true solution is periodic anyway. Likewise the chaos when  $G = 1.2$  is

clearly computational, but the question arises as to whether the similar chaos when  $G = 1.1$  or  $1.3$  should be called CC, since the true solutions are chaotic anyway. We shall leave these questions of terminology unanswered.

In preparing L06, we might well have chosen to speed the computations by using a somewhat longer time increment, possibly near  $0.037$ ; with the fourth-order differencing scheme the attractors would not have been noticeably changed. The reviewer would then have found the patently strange attractor of Fig. 3a, and, although probably noticing the imperfect resemblance to our attractor, would not have encountered a stable limit cycle, and might not have considered the differences in the details of the attractors worth mentioning. We would then never have been led to investigate the numerical solutions produced by first-order differencing. We would never have encountered CP, and we would not be preparing this article.

### 3. Higher-order differencing

Although the extremely small value of  $\tau_1$  apparent in Fig. 2b might not have been anticipated, it should surprise no one that first-order differencing schemes often do not constitute close approximations to the DEs. Here we examine the degree of improvement afforded by higher-order schemes. We find that CP is by no means eliminated.

Figure 5 shows the variations of  $\lambda_1$ ,  $\lambda_2$  and  $\lambda_3$  with  $\tau$ , in the manner of Fig. 2a, for successively increasing orders. When  $N = 2$  or 3, the range of  $\tau$  where CP occurs far exceeds the range where the true chaos is captured. Even with  $N = 4$  the ranges are

about equal. Only when  $N$  reaches 6 does CP almost disappear. We have found, however, that for each value of  $N$ , with  $\tau$  not too far below  $\tau_1$ , the numerically determined attractor closely resembles the true one.

It also appears from Fig. 5 that, once  $N > 2$ ,  $\tau_2$  shows little further systematic increase. We have found that  $\tau_2 = 0.35$  when  $N = 10$  and  $\tau_2 = 0.46$  when  $N = 20$ . We even integrated eqs. (1) with a 100th-order scheme—generally an impractical and useless undertaking—and found CI when  $\tau$  reached 0.53. Choosing an arbitrarily large  $N$  will not produce an arbitrarily large  $\tau_2$ , since in general the Taylor series do not converge when the argument is large.

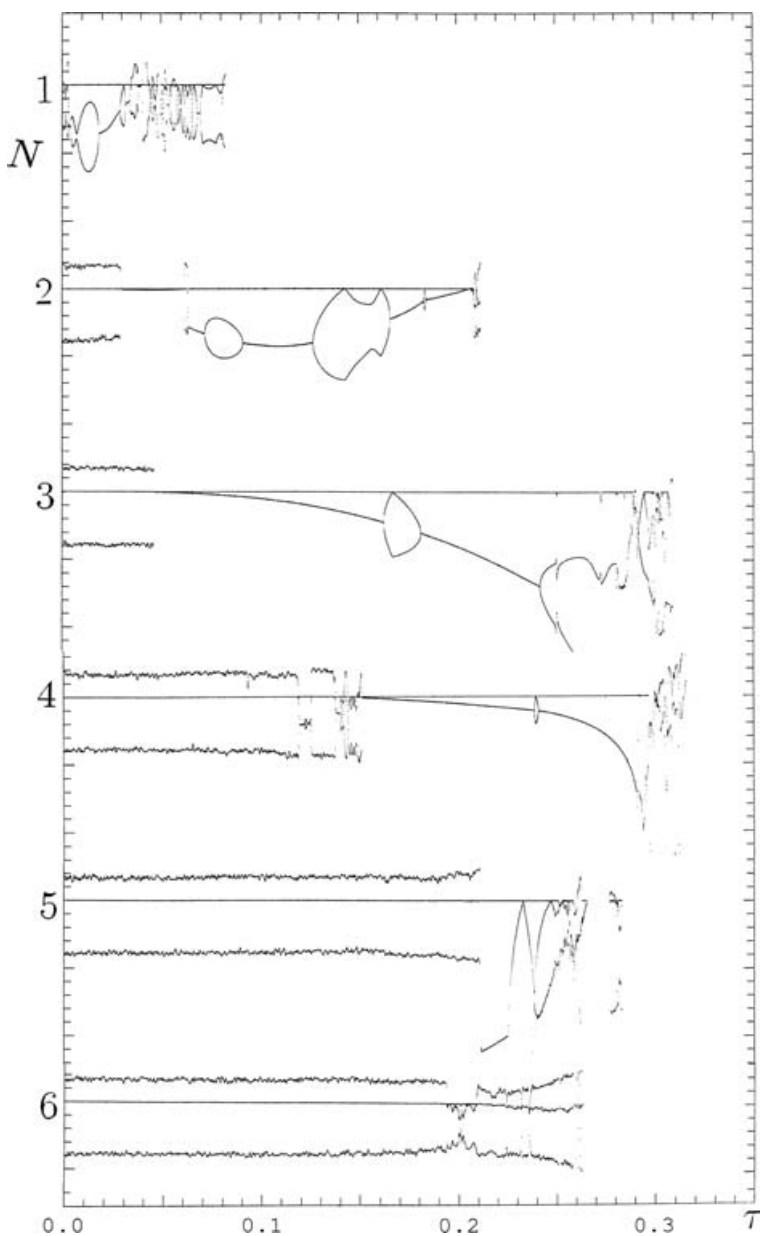


*Fig. 5.* The same as Fig. 2a, but separately for each order  $N$  of differencing scheme indicated by number at left of curves. Numbers indicating  $N$  are placed opposite zero lines for  $\lambda$ . Small divisions on left and right margins are at intervals of 0.1 unit of  $\lambda$ .

The Taylor-series scheme and the Runge–Kutta scheme are not the same (unless  $N = 1$ ), and one might wonder whether the results shown in Fig. 5 are peculiar to the former. We have repeated the computations of  $\lambda_1$ ,  $\lambda_2$ , and  $\lambda_3$  with a fourth-order Runge–Kutta scheme. Qualitatively we find little change from Fig. 5, but  $\tau_1 = 0.11$  rather than 0.14, and  $\tau_2 = 0.49$  rather than 0.33, so that the range of  $\tau$  where CP prevails is about twice as great. For good measure we have also applied the Adams–Bashforth scheme with  $N = 4$  to eqs. (1), and we find that  $\tau_1 = 0.048$  and  $\tau_2 = 0.085$ —great reductions from the values encountered with the other methods. Also, while this scheme is very fast, it is less convenient for tasks like evaluating Lyapunov exponents, where an initial state is perturbed and the consequences are observed, since the  $N$ th-order scheme uses  $N - 1$  past time derivatives for the forward extrapolation, and initially these must be perturbed consistently with the present state.

#### 4. Further considerations

An American writer once denounced the exhortation ‘See America first’ that was often proclaimed by the local vacation industry. He maintained that Americans could not see America without travelling to other countries and experiencing their way of life, thereby perhaps discovering that certain practices that they had always thought were universal were in fact peculiar to their own land. In a rather similar manner, even though our main interest is in the response of eqs. (1) to various differencing procedures, we may better appreciate our findings by examining the responses of some other equations.

We first choose the system

$$\frac{dx}{dt} = -y - z, \tag{3a}$$

$$\frac{dy}{dt} = x + ay, \tag{3b}$$

$$\frac{dz}{dt} = b + xz - cz, \tag{3c}$$

introduced by Rössler (1976) as a model of a chemical reaction. Containing a single quadratic term and no other non-linearities, it may well be the simplest set of autonomous DEs capable of producing chaos. Rössler found chaos with  $a = 0.2$ ,  $b = 0.2$  and  $c = 5.7$ , among other sets of values.

We have performed computations like those leading to Fig. 5, with  $N = 1, 2$ , and 3, for eqs. (3) with Rössler’s values of the constants. Again CP appears when  $N = 1$  or 2, although it occupies a smaller fraction of the range of  $\tau$  below  $\tau_2$ , and when  $N = 3$  it has disappeared. Also, as with eqs. (1), there is sometimes a range of  $\tau$  below  $\tau_2$  where CI occurs.

Next is the system of  $M$  equations

$$\frac{dX_m}{dt} = -X_{m-2}X_{m-1} + X_{m-1}X_{m+1} - X_m + F, \tag{4}$$

with  $X_{m+M} = X_m$ ; it has been used in a number of meteorological studies (e.g., Lorenz and Emanuel, 1998, Hansen and Smith, 2000, Hunt et al., 2004), where it simulates the variations of some quantity at  $M$  equally spaced points about a latitude circle.

With  $M > 4$ , chaos is fully developed whenever  $F > 8.0$ . With such combinations of values of  $M$  and  $F$  we have been unable to discover any instances of CP. In fact, we encountered CP only with  $M = 8$  or 9, and with  $F$  in a narrow range close to 4.0, where the chaos is incipient rather than fully developed.

A property distinguishing eq. (4) with  $F > 8$  from eqs. (1) and (3) and the special cases of eq. (4) is that the chaos occurring in the latter cases appears to be less robust, in the sense that relatively small changes in the values of one or more constants can remove the chaos, replacing it with periodicity. On the other hand, chaos can also be replaced by periodicity, if CP is present, by changing the value of  $\tau$ . If, for a given system, changes in  $\tau$  are qualitatively like changes in the constants, CP should be expected if the chaos produced by that system is not very robust.

That changing  $\tau$  and changing the constants have somewhat similar effects is suggested by the previously noted similarity between Fig. 1b, where the constants have been altered from those of Fig. 1a, and Fig. 3b, where  $\tau$  has been changed from Fig. 3a. Further support for this idea comes from Fig. 6, which shows the variations of the Lyapunov exponents of the DEs as the constants vary linearly through the values used in Fig. 1a and those in Fig. 1b, whence, as  $b$  varies,  $F = 6b - 16$  and  $G = F/8$ . The curves look familiar. With slight alterations they could be segments of a panel in Fig. 2 or 4, produced by varying  $\tau$ . Still another similarity is the intransitivity produced by some values of the constants; the periodicity in Fig. 6 when  $3.89 < b < 3.98$  would be replaced by chaos if different initial states were used in the computations.

With its frequent alternations between periodicity and chaos, Fig. 6 also supports our statement that the chaos produced by eqs. (1) lacks robustness. The appearance of CP in Figs. 2 and 4 should therefore not surprise us.

#### 5. Concluding remarks

This study has been concerned with the appearance of periodic numerical solutions of a system of equations whose exact solution is chaotic. It does not aim to establish theorems regarding the general properties of CP, although it includes a suggestion that CP is favoured when the chaos in the exact solution lacks robustness. Its limited findings may nevertheless have some practical implications.

The findings are based mainly on the evaluation of Lyapunov exponents. These, like attractors and the presence of periodicity or chaos, are long-term properties. Two systems that are rather similarly defined, such as the systems obtained by successively letting  $\tau$  equal 0.0038 and 0.0037 in the first-order approximation to eqs. (1), can be expected to yield rather similar short-range

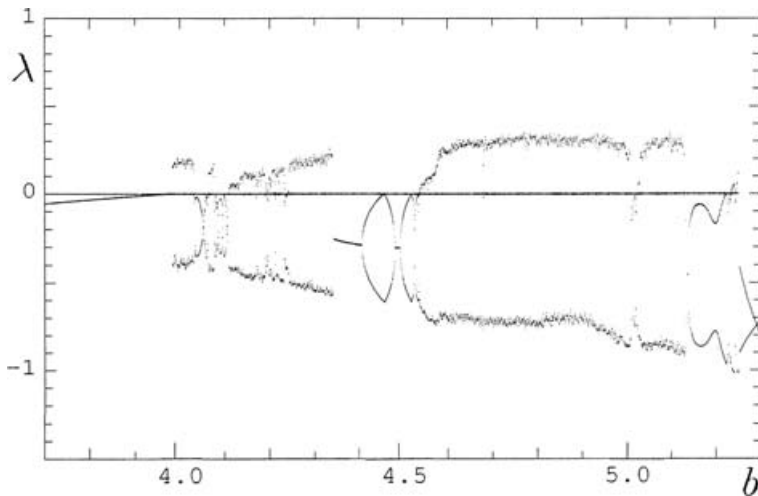


Fig. 6. Superposition of three curves showing variations with  $b$ , as  $b$  increases from 3.7 to 5.3 and  $F = 6b - 16$  and  $G = F/8$ , of Lyapunov exponents  $\lambda_1$ ,  $\lambda_2$  and  $\lambda_3$  of eqs. (1) when  $a = 1/4$ , as approximated by fourth-order Taylor-series procedure with  $\tau = 0.025$ . Horizontal coordinate is  $b$ . Vertical coordinate is  $\lambda$ .

forecasts from the same initial state, even though one may eventually attain periodicity while the other produces chaos.

For one whose main interest is large operational weather-forecasting models, our findings may be somewhat irrelevant. Presumably the differencing schemes there have been chosen to be compatible with the equations—effectively they are a part of the equations—and, I would assume, their properties will have been thoroughly examined. I must point out, however, that one reviewer finds my assumption far too optimistic.

Someone working instead with a simple model will more likely choose a simple differencing scheme. Even small computers are now so fast that millions of iterations can often be performed in a few seconds, but studies involving large ensembles or many sets of parameter values can still be time consuming, and the temptation to choose a rather large time increment  $\tau$  is always present. Our work suggests that such a choice is often quite legitimate, provided that it is accompanied by a bit of caution.

Suppose, for example, that you are simulating an entire short-range and medium-range operational weather forecasting routine, using simple equations, perhaps to investigate the effect of substituting a new data-assimilation scheme. You choose one set of DEs to simulate the truth, from which the simulated observations, with or without added errors, will be produced. You choose another set, or perhaps the same one with different values of the constants, to simulate the operational model. The chosen time increment qualifies as one of these constants.

Since simple DEs cannot closely approximate the real atmosphere in any event, there is no real reason why the output of your ‘truth’ system, with its chosen differencing scheme and time increment, needs to resemble that of the DEs used in obtaining it. Even something like the first-order approximation that produces Figs 3a or b may be acceptable. What is important is that you know the properties of your system. These may differ from those of the DEs, that have perhaps already been documented, and that you may wish your system to possess. In particular,

CP, with its consequent virtually infinite range of predictability, must be avoided. If your system includes seasonal variations of the constants, robustness may be an additional consideration.

As for the ‘operational’ system, its long-term properties, including the presence or absence of CP, are of minor concern. Since our findings pertain only to long-term behaviour, they are unlikely to add to the considerations that will determine your choice. If, however, you are simulating climate prediction rather than prediction at short or medium range, the long-term properties of your operational system, and their resemblance to those of the truth system, become essential considerations.

Meanwhile, dynamical systems exhibiting CP can be of interest for their own sake. The pattern of alternations between equal and unequal values of  $\lambda_2$  and  $\lambda_3$ , as  $\tau$  varies, prominent in Figs. 2 and 4, often possesses an intricate structure. Possibly one of these systems could form the basis for a unique study of bifurcation. Finally, the chaotic ranges that appear between separate ranges of CP can yield unusual attractors that may not be the exact attractors of any simple DEs. The nested attractors of Fig. 3 seem to be good candidates for further study.

## 6. Acknowledgments

I am greatly indebted to an anonymous reviewer of a previous article, whose attempt to duplicate some of my numerical results has led to the present investigation of the effects of differencing schemes on computed solutions. This work has been supported by the Large-Scale Dynamic Meteorology Program, Lower Atmosphere Research Section, Division of Atmospheric Sciences, National Science Foundation, under Grant ATM-0216866.

## References

- Aires, F. and Rossow, W. B. 2003. Inferring instantaneous, multivariate and nonlinear sensitivities for the analyses of feedback processes in a dynamical system: Lorenz model case study. *Q. J. R. Meteor. Soc.* **129**, 239–275.

- Courant, R., Friedrichs, K. O. and Lewy, H. 1928. Über die partiellen Differenzgleichungen der mathematische Physik. *Math. Ann.* **100**, 32–74.
- Durrant, D., 1999. *Numerical Methods for Wave Equations in Geophysical Fluid Dynamics*. Springer, New York, 465 pp. See p. 68.
- Giraldo, F. X., 2005. Semi-implicit time-integrators for a scalable spectral element atmospheric model. *Q. J. R. Meteor. Soc.* **131**, 2431–2474.
- Hansen, J. A. and Smith, L. A., 2000. The role of operational constraints in selecting supplementary observations. *J. Atmos. Sci.* **57**, 2859–2871.
- Hunt, R. R., Kalnay, E., Kostelich, E. J., Ott, E., Patil, D. J. and co-authors. 2004. Four-dimensional ensemble Kalman filtering. *Tellus* **56A**, 273–277.
- Lorenz, E. N., 1984. Irregularity: a fundamental property of the atmosphere. *Tellus* **36A**, 98–110.
- Lorenz, E. N., 1989. Computational chaos—a prelude to computational instability. *Physica D* **35**, 299–317.
- Lorenz, E. N., 2006. An attractor embedded in the atmosphere. *Tellus* **58A**, 291–296.
- Lorenz, E. N. and Emanuel, K. A. 1998. Optimal sites for supplementary weather observations: simulation with a small model. *J. Atmos. Sci.* **55**, 399–414.
- Rössler, O. E. 1976. An equation for continuous chaos. *Phys. Lett.* **57A**, 397–398.
- Trevisan, A. 1993. Impact of transient error growth on global average predictability. *J. Atmos. Sci.* **50**, 1016–1025.
- von Karman, T. and Biot, M. A. 1940. *Mathematical Methods in Engineering*. McGraw-Hill, New York, 505 pp.